



Ibuprofen-loaded poly(trimethylene carbonate-co- ϵ -caprolactone) electrospun fibres for nerve regeneration

Liliana R. Pires^{1,2}, Vincenzo Guarino³, Maria J. Oliveira^{1,4}, Cristina C. Ribeiro^{1,5}, Mário A Barbosa^{1,2,6}, Luigi Ambrosio³ and Ana Paula Pêgo^{1,2,6*}

¹INEB–Instituto de Engenharia Biomédica, NEWTherapies Group, Universidade do Porto, Porto, Portugal

²Universidade do Porto, Faculdade de Engenharia, Porto, Portugal

³Institute of Composite and Biomedical Materials, National Research Council, Naples, Italy

⁴Departamento de Patologia e Oncologia, Faculdade de Medicina, Universidade do Porto, Porto, Portugal

⁵ISEP–Instituto Superior de Engenharia do Porto, Instituto Politécnico do Porto, Porto, Portugal

⁶Universidade do Porto, Instituto de Ciências Biomédicas Abel Salazar, Porto, Portugal

*Correspondence to: A. P. Pêgo, INEB–Instituto de Engenharia Biomédica, NEWTherapies Group, Universidade do Porto, Rua do Campo Alegre 823, 4150-180 Porto, Portugal. E-mail: apegop@ineb.up.pt

Originally published in *J Tissue Eng Regen Med.* 2016 Mar;10(3):E154-66. doi: 10.1002/term.1792

"This is the peer reviewed version of the following article: *J Tissue Eng Regen Med.* 2016 Mar;10(3):E154-66, which has been published in final form at doi: 10.1002/term.1792. This article may be used for non-commercial purposes in accordance with Wiley Terms and Conditions for Use of Self-Archived Versions."

ABSTRACT

The development of scaffolds that combine the delivery of drugs with the physical support provided by electrospun fibres holds great potential in the field of nerve regeneration. Here it is proposed the incorporation of ibuprofen, a well-known non-steroidal anti-inflammatory drug, in electrospun fibres of the statistical copolymer poly(trimethylene carbonate-co- ϵ -caprolactone) [P(TMC-CL)] to serve as a drug delivery system to enhance axonal regeneration in the context of a spinal cord lesion, by limiting the inflammatory response. P(TMC-CL) fibres were electrospun from mixtures of dichloromethane (DCM) and dimethylformamide (DMF). The solvent mixture applied influenced

INSTITUTO
DE INVESTIGAÇÃO
E INOVAÇÃO
EM SAÚDE
UNIVERSIDADE
DO PORTO

Rua Alfredo Allen, 208
4200-135 Porto
Portugal
+351 220 408 800
info@i3s.up.pt
www.i3s.up.pt

Version: Postprint (identical content as published paper) This is a self-archived document from i3S – Instituto de Investigação e Inovação em Saúde in the University of Porto Open Repository For Open Access to more of our publications, please visit <http://repositorio-aberto.up.pt/>

fibre morphology, as well as mean fibre diameter, which decreased as the DMF content in solution increased. Ibuprofen-loaded fibres were prepared from P(TMC-CL) solutions containing 5% ibuprofen (w/w of polymer). Increasing drug content to 10% led to jet instability, resulting in the formation of a less homogeneous fibrous mesh. Under the optimized conditions, drug-loading efficiency was above 80%. Confocal Raman mapping showed no preferential distribution of ibuprofen in P(TMC-CL) fibres. Under physiological conditions ibuprofen was released in 24 h. The release process being diffusion-dependent for fibres prepared from DCM solutions, in contrast to fibres prepared from DCM-DMF mixtures where burst release occurred. The biological activity of the drug released was demonstrated using human-derived macrophages. The release of prostaglandin E₂ to the cell culture medium was reduced when cells were incubated with ibuprofen-loaded P(TMC-CL) fibres, confirming the biological significance of the drug delivery strategy presented. Overall, this study constitutes an important contribution to the design of a P(TMC-CL)-based nerve conduit with anti-inflammatory properties.

Keywords confocal Raman microscopy; drug delivery; electrospinning; ibuprofen; inflammation; nerve guide

1. INTRODUCTION

The first patent on electrospinning dates from 1934 by Formhals ([1934](#)). More recently, the technique was 'reinvented', becoming very popular for the preparation of tissue engineering scaffolds (Martins *et al.*, [2007](#); Agarwal *et al.*, [2009](#)). Electrospinning allows the fabrication of nanofibrous scaffolds that can emulate the extracellular matrix, providing a biomimetic environment for cell growth, polarization and differentiation. In addition, a number of parameters in the electrospinning setup can be adjusted in order to modulate fibre diameter and orientation, as well as scaffold size and shape. The possibility of preparing aligned fibres has been especially explored in the context of nerve repair (Xie *et al.*, [2010](#); Lee and Arinze, [2011](#)). Previous reports show that neurons align their cellular processes in the direction of electrospun fibres *in vitro* (Corey *et al.*, [2007](#); Yao *et al.*, [2009](#)). A similar outcome was observed *in vivo*, both in the peripheral (Yu *et al.*, [2011](#); Jiang *et al.*, [2012](#)) and in the central nervous system (Hurtado *et al.*, [2011](#)). Electrospun scaffolds can also serve as drug delivery devices. Owing to the versatility of the electrospinning technique, different types of molecules can be incorporated in fibres. For nerve regeneration applications, fibres have been loaded with neurotrophins (Chew *et al.*, [2005](#); Liu *et al.*, [2012](#)) or drugs, like 6-aminonicotinamide, known to limit astrocyte proliferation (Schaub and Gilbert, [2011](#)). To promote central nervous system regeneration, the combination of nanofibrous scaffolds with molecules that can locally hinder the inhibitory environment after a lesion is of particular interest (Liu *et al.*, [2012](#)).

Inflammation is one of the secondary events activated after a central nervous system lesion and one of the most relevant targets in nerve regeneration strategies (Thuret *et al.*, [2006](#); Fitch and Silver, [2008](#)). Although the role of inflammation in central nervous system regeneration is currently an issue of active debate (Chan, [2008](#); Schwartz *et al.*, [2009](#)), the results of clinical trials that involved assessment of drugs with described anti-inflammatory properties, namely the antibiotic minocycline (Casha *et al.*, [2012](#)), support strategies targeting the modulation of the inflammatory response.

This report proposes the incorporation of ibuprofen in electrospun fibres as a drug delivery system to enhance axonal regeneration in the context of a spinal cord lesion by limiting the inflammatory

response. Ibuprofen is a non-steroidal anti-inflammatory drug and its action is attributed to the inhibitory effect on cyclooxygenase (COX). This enzyme is responsible for the conversion of arachidonic acid in prostaglandins, the latter being associated with pain, fever and acute inflammatory reaction (Mitchell *et al.*, 1993; Rainsford, 2009). In addition to the classical view of the action of ibuprofen, the release of prostaglandin E₂ (PGE₂) has been more recently associated with neuropathic pain after spinal cord injury (Zhao *et al.*, 2007). Consequently, targeting the COX pathway is currently indicated as a new avenue to treat this condition (Ma *et al.*, 2012), providing added value to the strategy proposed in this manuscript.

Poly(trimethylene carbonate-co- ϵ -caprolactone) [P(TMC-CL)] is a biodegradable elastomer previously studied in the field of nerve regeneration research. The polymer possesses mechanical properties and a degradation profile appropriate to serve as nerve conduit (Pêgo *et al.*, 2001, 2003) and it has shown to be able to support peripheral nerve regeneration *in vivo* (Vleggeert-Lankamp *et al.*, 2008). In the present work, it is proposed that P(TMC-CL) serve as polymeric matrix for the delivery of ibuprofen. The optimization of electrospun P(TMC-CL) fibre preparation, the incorporation of the drug and its release profile and bioactivity are investigated.

2 Materials and methods

2.1 Polymer synthesis

Poly(trimethylene carbonate-co- ϵ -caprolactone) was prepared by ring-opening polymerization as previously described (Pêgo *et al.*, 2001). In brief, ϵ -caprolactone (CL) (Merck, Darmstadt, Germany) was dried overnight (calcium hydride; Sigma-Aldrich Química, Sintra, Portugal) and distilled before the polymerization with trimethylene carbonate (TMC, used as received from Boehringer Ingelheim, Ingelheim am Rhein, Germany). Polymerization was carried out in evacuated and sealed glass ampoules using stannous octoate (Sigma-Aldrich) as catalyst (2×10^{-4} mol per mol of monomer). After 3 days of reaction at 130 °C the polymer obtained was purified by dissolution in chloroform (BDH-Prolabo, Carnaxide, Portugal) and subsequent precipitation into a tenfold volume of ethanol (96%, v/v; AGA, Prior Velho, Portugal). The chemical composition of the copolymer was assessed by ¹H nuclear magnetic resonance (NMR) and found to contain 11% mol of TMC, which is in accord with the monomer ratio charged (10% mol TMC). The molecular weight of the obtained polymer was determined by size exclusion chromatography using chloroform as the mobile phase. The average molecular weight was found to be 8.2×10^4 g/mol and the polydispersity index was 1.61.

2.2 P(TMC-CL) and ibuprofen-loaded P(TMC-CL) fibre preparation by electrospinning

Initially, a range of electrospinning parameters was assessed. The parameters tested included polymer concentration in the electrospun solution (6–10%, w/v), polymer solvent [dichloromethane (DCM; Merck), chloroform (Sigma-Aldrich) and *N,N*-dimethylformamide (DMF, Merck)], flow rate (0.1–1.5 ml/h), and electric field applied (0.5–1 kV/cm). Based on the morphology of the fibres obtained (data not shown) the selected conditions for the subsequent experiments were: P(TMC-CL) solutions (10%, w/v) dispensed at a flow rate of 1 ml/h using a syringe pump (Ugo Basile, Italy); an electric field (Gamma High Voltage source; Ormond Beach, FL, USA) of 1 kV/cm applied between the spinneret (inner diameter 0.8 mm) and a flat copper plate (15 × 15 cm) separated by 14 cm; DCM and DMF mixtures used as solvent at the volume ratios of 1:0, 6:1, 3:1 and 1:1. Fibres were collected into

an aluminium foil for 1–1.5 h. After vacuum drying (vacuum oven, Raypa, Barcelona, Spain) for 24 h, 14 mm discs were punched out from the electrospun membranes and stored at room temperature (20–25 °C) until further use.

Ibuprofen-loaded fibres were obtained by adding 5% and 10% of ibuprofen powder (w/w of polymer) to the polymer solution 5 h before electrospinning. Pharmaceutical grade ibuprofen (purity > 99%) was kindly supplied by Sérgio Simões (Bluepharma, Coimbra, Portugal).

2.3 Fibre characterization

2.3.1 Fibre morphology

Fibre morphology was analysed by scanning electron microscopy (SEM). A low vacuum (5 kV) Phenom™ G2 (Phenom-World, Eindhoven, the Netherlands) and a Quanta 400FEG ESEM (FEI, Eindhoven, the Netherlands) microscopes were used. Fibre diameter was quantified from SEM micrographs using image analysis software (Image J, version 1.39; NIH, Bethesda, MD, USA). Fibre mean diameter and fibre diameter distribution were calculated from at least 100 measurements from three independent samples.

2.3.2 Drug loading efficiency

¹H NMR spectroscopy was used in order to quantify ibuprofen in the P(TMC-CL) electrospun meshes. The analyses were performed in an AVANCE III 400 spectrometer (Bruker Corporation, Barcelona, Spain), operating at 400 MHz. The ¹H chemical shifts were internally referenced to the tetramethylsilane (TMS; Eurisotop, Saint-Aubin, France) signal (0.00 ppm) for spectra recorded in CDCl₃ (Sigma-Aldrich). Ibuprofen-loaded P(TMC-CL) fibres were dissolved in CDCl₃ before analysis. Characteristic peaks from ibuprofen and P(TMC-CL) were used to identify both species. The drug loading efficiency was calculated from the ratio between the area of the signal at $\delta = 2.45$ ppm corresponding to the CH₂ group of ibuprofen (2H), and the area of the peak corresponding to the resonance of the α -methylene ($\delta = 2.30$, 2H, CH₂) of polymeric caprolactone.

2.3.3 Ibuprofen distribution in P(TMC-CL) fibres

Ibuprofen powder and P(TMC-CL) fibres prepared from 1:0 and 3:1 DCM–DMF mixtures with and without ibuprofen incorporated (5%, w/w, of polymer) were analysed using Fourier transform infrared spectroscopy (FTIR) and confocal Raman microscopy.

The FTIR characterization was performed using a Perkin Elmer 2000 spectrometer (Perkin Elmer, Waltham, MA, USA) and an attenuated total reflectance (ATR) accessory (SplitPea™; Harrick Scientific, Pleasantville, NY USA), provided with a silicon internal reflection element and configured for external reflectance mode, where the spectra were acquired from a 200 μ m diameter sampling area. A nitrogen purge was performed before each experiment. All samples were run at a spectral resolution of 4/cm and 200 scans were accumulated in order to obtain a high signal-to-noise level. The band at 1675–1775/cm was deconvoluted by applying the derivative and curve fitting algorithms using peakfit from AISN Software (Florence, Oregon, USA). Initial peak positions were obtained from second derivative spectra of the raw data. A Lorentzian band-shape was used to fit the contours.

Confocal Raman microscopy analyses were performed using a LabRAM HR 800 confocal Raman microscope system (Horiba Jobin Yvon, Lille, France) comprising a spectrometer and a fully integrated Olympus BX41 confocal microscope (Olympus Iberia, S.A.U., Lisboa, Portugal). Raman spectra were generated using a 514 nm laser diode as excitation source, focused on the sample with a $\times 100$ objective, a confocal hole of 100 μm and an exposure time of 100 s. For the experimental setup used, the spatial resolution is between 0.5 μm and 1 μm . The scattered light was dispersed by a grating with 1800 lines/mm (Jobin-Yvon) at 4/cm spectral resolution. Spectral analysis was carried out using labspec5 software (Horiba Jobin Yvon). Imaging experiments on fibres were performed by scanning the laser beam over the region of interest and accumulating a full Raman spectrum at each pixel. Raman images were constructed by plotting the integrated intensity of the vibrational bands of interest as a function of position. For these experiments, fibres with a diameter $> 2 \mu\text{m}$ were selected and step size for data acquisition was approximately 0.6 μm . The spectral range measured was 1400–1800/cm and the mapping area varied according to the fibre dimension.

2.4 Drug-release studies

The amount of ibuprofen released from the electrospun P(TMC-CL) fibres was evaluated as follows. Samples loaded with 5% of ibuprofen (w/w of polymer) were incubated at 37 °C and 120 rpm (Orbital Shaker Oven; IKA, Staufen, Germany) in phosphate buffered saline (PBS) at the final concentration of 5 mg/ml (mass of fibres/volume of PBS). At defined time-points (0.5, 1, 2, 4, 6, 8, and 24 h) the releasing medium was refreshed. Ultraviolet/visible spectroscopy (UV/Vis) at 230 nm (SynergyMx; Biotek, Carnaxide, Portugal) was used to monitor the amount of ibuprofen released. Values were interpolated from an ibuprofen calibration curve (see the Supporting Information, Figure S4). Cumulative release was calculated relative to the maximum loading of 5% (w/w of polymer). The drug release kinetics was analysed using the Higuchi simplified model:

$$M_t/M_\infty = k\sqrt{t} \quad (1)$$

Where M_t/M_∞ represents cumulative ibuprofen release, t is time of incubation and k is a constant reflecting the design variables of the system (Siepmann and Peppas, 2001).

2.5 Biological effect of ibuprofen on human macrophages

2.5.1 Peripheral blood-derived monocyte isolation

Human peripheral blood-derived monocytes were isolated from Buffy coats (kindly donated by Instituto Português do Sangue, Porto, Portugal) by negative selection using Rosettesep™ (StemCell Technologies, Grenoble, France) as previously described (Oliveira *et al.*, 2012). A day after isolation, adherent cells were collected applying a 5 mm solution of ethylenediamine tetraacetic acid (EDTA; BDH-Prolabo) and reseeded on glass coverslips at a cell density of 1.25×10^5 cells/cm². The cell population contained $> 70\%$ of CD14 positive cells and no contamination by CD3-positive T lymphocytes, as determined by flow cytometry (Oliveira *et al.*, 2012). Cells were allowed to differentiate in RPMI medium (Gibco, Life technologies S.A., Madrid, Spain) supplemented with 10% of heat-inactivated (56 °C, 30 min) fetal bovine serum (Lonza, Barcelona, Spain) for additional 8 days. Ten days after isolation, monocyte-derived macrophages were stimulated with 10 ng/ml lipopolysaccharide (LPS; Sigma) for 72 h. Specific cell treatments were performed after LPS activation.

2.5.2 Cell culture

The effect of ibuprofen on macrophage metabolic activity was assessed by means of a resazurin-based assay. In brief, different ibuprofen solutions in ethanol–water mixtures (7:3) were prepared and added (5 µl) to the cell culture media (500 µl) in order to obtain a final drug concentration ranging from 0.001 mg/ml to 1 mg/ml. Cell metabolic activity was evaluated at 24 h and 72 h after treatment. At the defined time-point cells were incubated (4 h, 37 °C) with a resazurin (Sigma-Aldrich) solution (0.1 mg/ml, in PBS) and the fluorescence ($\lambda_{ex} = 530$ nm, $\lambda_{em} = 590$ nm) in the cell culture medium was measured (SynergyMx; Biotek). Results are represented as percentage of cell viability relative to cells treated with equal volume of the ibuprofen solvent (5 µl).

In order to evaluate the bioactivity of ibuprofen released from P(TMC-CL) electrospun fibres, fibre discs (14 mm) were incubated with macrophages for 72 h. The fibres tested were prepared from 1:0 DCM–DMF solutions loaded with 5% ibuprofen (w/w of polymer). The punched discs weighed between 0.9 mg and 3 mg. Fibre sterilization was performed by irradiating (gamma rays, 25 kGy, ^{60}Co source) samples previously packed under vacuum. Fibre discs were suspended in the well without direct contact with the cells. Macrophages treated with ibuprofen in the medium (final concentration 0.1 mg/ml), as well as cells cultured in presence of unloaded P(TMC-CL) fibres, were used as control.

2.5.3 Immunofluorescence

To analyse cell morphology, macrophages were fixed with 4% (w/v) paraformaldehyde (Merck) and immunostained for α -tubulin and F-actin as follows. Cell external fluorescence was quenched by treating the cells with 50 mM NH_4Cl for 10 min. Subsequently, cells were permeabilized with 0.1% (v/v) Triton X-100 (in PBS) for 5 min. After washing with PBS, cells were incubated with 5% (w/v) bovine serum albumin (BSA; Sigma-Aldrich) in PBS for 30 min and, thereafter, incubated with the primary antibody mouse anti- α -tubulin (1:4000; Sigma-Aldrich) for 1 h. Subsequently, cells were thoroughly washed and incubated with Alexa Fluor 594 goat anti-mouse IgG (1:1000; Invitrogen, Life technologies Madrid, Spain) for 45 min. F-actin was stained for 15 min using 5 µm Phalloidin-FITC (Sigma-Aldrich). Cells were washed with PBS and mounted on Vectashield with 4',6-diamidino-2-phenylindole (DAPI; Vector Laboratories, Peterborough, UK). Samples were observed under an inverted fluorescence microscope (Axiovert 200; Zeiss, Oberkochen, Germany).

2.5.4 PGE₂ and quantification of cytokines

At the defined time-point (72 h after treatment), cell culture supernatants were collected and, after centrifugation (16000 g, 4 °C, 10 min) to remove cell debris, stored at –20 °C for posterior analysis. The concentration in the cell culture supernatant of PGE₂ (Cayman Chemical, Ann Arbor, MI, USA), interleukin 6 (IL-6), IL-10 and tumour necrosis factor- α (TNF α) were quantified by enzyme-linked immunosorbent assay (ELISA; Biologend, San Diego, CA, USA) following the manufacturer's instructions. Results are presented normalized for the total protein content in the cell culture medium, as determined by the DC protein assay (Bio-Rad, Amadora, Portugal).

2.6 Statistical analysis

Statistical analysis was performed using prism 5.0 software (GraphPad, La Jolla, CA, USA). Statistical differences between two groups were calculated applying a *t*-test when analysing results from PGE₂

and release of cytokines. Mean fibre diameters obtained when using different solvent combinations loaded or unloaded with ibuprofen were analysed using non-parametric Kruskal–Wallis test and Bonferroni correction for multiple comparisons. A p -value lower than 0.05 was considered statistically significant.

3 Results

3.1 Characterization of P(TMC-CL) and ibuprofen-loaded P(TMC-CL) fibres

3.1.1 Fibre morphology

The influence of solvent composition on P(TMC-CL) fibre morphology was evaluated by testing different DCM–DMF mixtures (Figure 1, Table 1). Fibres prepared from 1:0 DCM–DMF solutions showed a broad diameter distribution. Improved homogeneity of the fibres was observed when increasing the DMF fraction in solution, as shown by the narrowing of the fibre diameter distribution (Figure 1). The fibre mean diameter was found to be $1.09 \pm 0.10 \mu\text{m}$ for fibres prepared from 1:0 DCM–DMF solutions, decreasing to $0.48 \pm 0.03 \mu\text{m}$ for fibres prepared from 1:1 DCM–DMF solutions (Table 1).

Ibuprofen-loaded P(TMC-CL) fibres were prepared by adding 5 % and 10 % of the drug (w/w of polymer) to the polymer solution before electrospinning. Electrospinning parameters applied were the same as those optimized for the preparation of the non-loaded fibres. When 5% of ibuprofen (w/w of polymer) was added to the P(TMC-CL) solution, smaller fibres were formed, as indicated by the decrease in mean fibre diameter in comparison with unloaded fibres (Table 1). When analysing the effect of the solvent composition on the morphology of 5% ibuprofen-loaded fibres, under the conditions tested, fibres prepared from 1:1 DCM–DMF solutions fused (Figure 2). For this reason, a 1:1 DCM–DMF solutions was not tested for 10% ibuprofen-loaded fibres. No significant differences in terms of mean fibre diameter were detected when comparing loaded fibres prepared from 1:0, 6:1 and 3:1 DCM–DMF solutions. However, in terms of fibre diameter distribution a higher percentage of bigger fibres ($> 3 \mu\text{m}$) were formed from 1:0 DCM–DMF solutions (Figure 2). When fibres were prepared from solutions with 10% ibuprofen (w/w of polymer), the high drug content led to jet instability, resulting in a less homogeneous fibre mesh. Under these conditions a tendency towards the formation of defects and large-diameter fibres was observed, as indicated by the fibre diameter distribution graphs (Figure 2), albeit the mean fibre diameter was not remarkably affected (Table 1). For fibres prepared from 3:1 DCM–DMF solutions, in particular, fusion of the deposited fibres was also observed.

3.1.2 Drug loading and distribution

The chemical composition of ibuprofen-loaded P(TMC-CL) fibres was analysed by means of three spectroscopic techniques: ^1H NMR, ATR-FTIR and Raman.

By ^1H NMR spectroscopy, ibuprofen was clearly distinguished from P(TMC-CL) signals (see the Supporting information, Figure S1). The amount of drug relative to the polymer was quantified using this technique. It was found that in the 5% ibuprofen (w/w of polymer) loaded P(TMC-CL) fibres the

actual loading was 4.21 ± 0.02 % (w/w of polymer; $n = 3$), corresponding to a loading efficiency of over 80%.

As NMR provides information about the bulk chemical composition of the prepared samples, to obtain complementary chemical characterization of the fibres, these were also analysed by ATR-FTIR. Figure 3A shows the spectra of ibuprofen-loaded P(TMC-CL) fibres prepared from 1:0 DMC-DMF solution, unloaded fibres and ibuprofen powder. The most intense bands of ibuprofen are located at 2955, 1721 and 1231/cm, being assigned to CH_3 asymmetric stretching, C = O stretching and C–C stretching, respectively (see full FTIR spectra in Figure S2). These bands cannot be distinguished in the ibuprofen-loaded fibres because of overlapping with the polymer signals. Although weak, the band corresponding to the aromatic C = C stretching vibration of ibuprofen (1509/cm) can be identified in the ibuprofen-loaded P(TMC-CL) fibre spectrum, confirming the presence of the drug in the fibres (Figure 3A). In order to identify the presence of subtle spectral changes in the region of the most intense bands of ibuprofen and P(TMC-CL) (1670–1800/cm) a second derivatization and curve fitting of the raw data was performed. Figure 3A(I,II) shows that the number of bands in that particular zone of the spectrum increases in the loaded polymer samples further supporting the presence of ibuprofen in the fibres. Analysis of the ibuprofen-loaded P(TMC-CL) spectrum compared with those of P(TMC-CL) and ibuprofen showed no differences other than the characteristic bands of the starting materials, suggesting that no chemical interaction between ibuprofen and the polymer occurred. ATR-FTIR analysis of P(TMC-CL) fibres prepared from 3:1 DCM-DMF solutions was also performed and similar spectra were obtained.

As a complementary technique to FTIR P(TMC-CL), individual fibres were analysed by confocal Raman spectroscopy. By using this technique it was possible to identify the C–C stretching (1610/cm) on the fingerprint region of ibuprofen (Figure 3B). The presence of this clear marker band allowed the use of Raman mapping to determine and compare the spatial distribution of ibuprofen in P(TMC-CL) fibres prepared with 1:0 and 3:1 DCM-DMF solutions. Data was acquired on an area of the fibre as shown in Figure 3C(I,DI). Mapping was performed by rationing the ibuprofen fingerprint region to the background signal in two different spectral regions: 1510–1525/cm and 1645–1665/cm. Regions with high concentration of ibuprofen are depicted in bright green, while regions with low ibuprofen concentration are shown in black (see Figure 3E). Although drug distribution is not completely homogeneous, results show no preferential distribution of the drug at fibre edges or in the centre for both ibuprofen-containing fibres prepared from 1:0 and 3:1 DCM-DMF P(TMC-CL) solutions (Figure 3 (CII,DI)).

3.2 Drug-release studies

The release of ibuprofen from P(TMC-CL) fibres was evaluated in PBS at 37 °C, to mimic physiological conditions. The amount of ibuprofen released was interpolated from a calibration curve and the percentage of cumulative release was calculated relative to the maximum loading of 5% (w/w of polymer).

Under the experimental conditions tested, ibuprofen was released from the P(TMC-CL) fibres within the first 24 h of incubation in PBS (37 °C), independently of the solvent mixture used for fibre preparation. None, or residual amounts of ibuprofen were detected in the releasing medium when loaded fibres were incubated for longer periods (data not shown). In the case of fibres prepared from 6:1 and 3:1 DCM-DMF solutions, a burst release appeared to occur (Figure 4B,C). In contrast, the

release kinetics of ibuprofen from fibres prepared in 1:0 DCM–DMF was slower, suggesting time-dependency (Figure 4A). Analysing ibuprofen release using the Higuchi model it was found that the release profile of ibuprofen from P(TMC-CL) fibres prepared from 1:0 DCM–DMF solutions fitted better in the model, indicating that the release is diffusion dependent for the first 8 h of incubation in PBS (see fitting curve in Figure S5). Observation of the fibres after the drug release experiments showed that fibre morphology was maintained upon drug release (Figure S6).

3.3 Biological evaluation

Ibuprofen anti-inflammatory properties have been associated to its inhibitory action on COX (Mitchell *et al.*, 1993). This enzyme is responsible for the formation of prostaglandins (such as PGE₂) from arachidonic acid, and is related with the inflammatory response (for a review see Rainsford, 2009). To ensure that the ibuprofen incorporated into the P(TMC-CL) fibres exerted its biological activity, the release of cytokines and PGE₂ by monocyte-derived human macrophages was quantified after incubating the cells with the fibers or soluble ibuprofen (positive control). Taking advantage of the fact that P(TMC-CL) density is similar to water density and consequently the discs hang in cell culture medium, the fibres were incubated without direct contact with the adhered cells. This set up made it possible to distinguish the effect of the drug from any effect triggered by the polymer surface, as macrophage response and differentiation is affected by surface chemistry (Brodbeck *et al.*, 2002), and by its topography (Cao *et al.*, 2010). In this study the aim was to discern the effect of the released drug regardless of cell–material interaction.

3.3.1 Effect of ibuprofen on macrophage cell viability and morphology

To assess ibuprofen cytotoxic profile on monocyte-derived human macrophages, the drug was added in its soluble form to the cell culture medium to a final concentration ranging from 0.001–1 mg/ml. Ibuprofen solvent (ethanol 70% v/v) was also applied as a negative control. The graph presented in Figure 5A indicates that, at the highest concentration tested (1 mg/ml), ibuprofen was toxic for macrophages, significantly reducing cell viability (< 10%). Similar results were obtained when cell metabolic activity was assessed 24 h post-treatment (data not shown). Taking into consideration these results, 0.1 mg/ml soluble of ibuprofen was applied in the following experiments as control.

The effect of ibuprofen-loaded P(TMC-CL) fibres on macrophage morphology was investigated by observing the distribution pattern of cytoskeleton proteins (α -tubulin and F-actin). Therefore, human primary macrophages were incubated for 72 h with soluble ibuprofen at a final concentration of 0.1 mg/ml, with ethanol (70% v/v, ibuprofen solvent), with P(TMC-CL) fibres or with ibuprofen-loaded P(TMC-CL) fibres. In all the experimental conditions tested macrophages showed evidence of heterogeneous cell morphology, with round-shaped cells and F-actin staining concentrated at the cell periphery in podosome-like structures, and elongated cells with less intense and peripheral F-actin staining. In contrast, α -tubulin staining was always homogeneously distributed along the cell body and according the cell axis (Figure 5). No significant differences in terms of macrophage morphology were observed between the different experimental conditions.

3.3.2 Anti-inflammatory properties of ibuprofen-loaded P(TMC-CL) fibres

To assess if the ibuprofen released from ibuprofen-loaded P(TMC-CL) electrospun fibres is bioactive, the concentration of soluble PGE₂ produced by exposed macrophages was quantified in the cell culture supernatants after 72 h of incubation.

The results (Figure 6) indicate that when ibuprofen is added to the medium the release of PGE₂ decreases, suggesting that COX is being inhibited. The same tendency is observed when comparing the effect of ibuprofen-loaded fibres and non-loaded fibres (Figure 6), although none of the differences achieved statistical significance. In terms of inhibition, considering the mean values, when ibuprofen is added in solution there is a 56% decrease in PGE₂ release, while ibuprofen released from P(TMC-CL) electrospun fibres can reduce the release of PGE₂ by 47%. However, when comparing the effect of ibuprofen released from P(TMC-CL) fibres directly with control conditions one should take into account that the amount of drug that can be released from P(TMC-CL) fibres is in a concentration range and can slightly differ from the control concentration used in this assay.

The effect of ibuprofen on the release of IL-6, IL-10 and TNF α was also evaluated. Under the experimental conditions of this study, ibuprofen was found to induce no significant effect on the release of IL-6 or IL-10 when added in solution or when released from electrospun P(TMC-CL) fibres (Figure 6). The concentration of TNF α secreted into the cell culture medium was found to be below the detection limit (3.5 pg/ml) of the ELISA assay (data not shown).

4 Discussion

The preparation of nerve conduits by electrospinning holds the promise of allowing easy preparation of fibres, at the nanometre scale, that can guide axonal growth and be loaded with biologically active molecules able to enhance nerve regeneration processes (Lee and Arinzeh, 2011). In the present work, the aim was to prepare fibres of a statistical copolymer of TMC and CL with low TMC content (11 mol%) by electrospinning and to load these with an anti-inflammatory drug. The idea beyond this strategy is to design scaffolds that can provide physical support for nerve cell growth, and that simultaneously minimize, at the lesion site, the inflammatory reaction that could counteract nerve regeneration. The preparation of electrospun structures based on a block copolymer of TMC and CL (Jia *et al.*, 2006) or blends of P(TMC) and P(CL) (Han *et al.*, 2010) have been reported in the literature. Nevertheless, a statistical copolymer holds the advantage of reducing the formation of crystalline domains and reducing phase separation within the polymer structure, which is desirable when envisaging the use of these materials in implantable devices (Pêgo *et al.*, 2001). The authors have previously reported on the use of selected statistical P(TMC-CL) for the preparation of microporous and macroporous conduits for nerve reconstruction in the peripheral nervous system. P(TMC-CL) with a high CL content has been shown to possess adequate mechanical properties and degradation rate to be used in a nerve regeneration strategy (Pêgo *et al.*, 2001, 2003), as it is able to support nerve regeneration *in vivo* (Vleggeert-Lankamp *et al.*, 2008). This paper describes for the first time the preparation of electrospun fibres from this copolymer.

By using different DCM–DMF mixtures in the electrospinning solution it was possible to prepare fibrous meshes with variable mean fibre diameter. Increasing the DMF content in solution, mean fibre diameter was decreased from 1.09 μm to 0.48 μm . DMF is a high conductivity solvent, and its use in the preparation of solutions for electrospinning leads to an increase in jet splaying and a reduction of fibre diameter (Hsu and Shivkumar, 2004). Typically, DMF is used below 30% in solution, as described for the preparation of fibres of P(CL) (Bölgen *et al.*, 2005) and P(CL)/P(TMC) blends (Han *et al.*, 2010).

Herein, the preparation of fibres from solutions containing up to 50% of DMF was explored. Results show that by increasing the DMF content one can obtain very homogeneous fibre meshes, with narrower fibre diameter distribution and smaller mean fibre diameter. However, the use of 1:1 DCM–DMF solutions was revealed to be unsuitable for the preparation of ibuprofen-loaded P(TMC-CL) fibres at the drug concentrations tested. It was previously described that the incorporation of drugs in electrospinning solutions can lead to an increase in solution conductivity (Kim *et al.*, 2004). This increase, combined with the high DMF content, may cause fibres to bind together because of the high conductivity (Heikkilä and Harlin, 2008) and high boiling point of DMF, which prevent solvent evaporation during fibre deposition (Hsu and Shivkumar, 2004).

Ibuprofen-loaded fibres were obtained from 1:0, 6:1 and 3:1 DCM–DMF mixtures. In terms of morphology, when applying a 5% of ibuprofen (w/w of polymer) load, a tendency towards a decrease in mean fibre diameter is observed compared with unloaded fibres. This effect is particularly noticeable for 1:0 DCM–DMF solutions, probably because the presence of the drug led to a more marked increase in solution conductivity compared with solutions containing DMF (Kim *et al.*, 2004). Although the differences in terms of mean fibre diameter are not significant, when loading 10% ibuprofen in solution, jet stability and solvent evaporation are reduced, the latter being particularly evident in the case of the 3:1 DCM–DMF solution. The increase in jet instability with higher drug loading has also been reported previously (Natu *et al.*, 2010).

The presence of ibuprofen in P(TMC-CL) fibres was clearly demonstrated by ATR-FTIR and Raman spectroscopy. Both techniques showed that the chemical stability of ibuprofen is maintained after electrospinning. In addition, no alterations in the characteristic peaks of P(TMC-CL) and ibuprofen are seen in ibuprofen-loaded P(TMC-CL) spectrum, indicating that there is no significant chemical interaction between the polymer and the drug, as previously observed in ibuprofen-loaded cellulose acetate fibres (Tungprapa *et al.*, 2007).

The ibuprofen release kinetics from P(TMC-CL) fibres were assessed in physiological medium (PBS, 37 °C). Results demonstrate that ibuprofen is released within the first 24 h after incubation in PBS, independently of the solvent mixture used for the preparation of the fibres. It was previously reported that the expression of cyclooxygenase-2 peaks 3 h after spinal cord injury (SCI), and is maintained for 3 days (Adachi *et al.*, 2005). In this context, the release of ibuprofen in the early hours after the lesion can provide the expected therapeutic benefit. A complete ibuprofen release in the first 24 h of incubation under physiological conditions has also been reported using cellulose acetate fibres (Tungprapa *et al.*, 2007). In terms of kinetics, we found an initial burst release for fibres prepared from 6:1 and 3:1 DCM–DMF mixtures. However, in the case of fibres prepared from 1:0 DCM–DMF the release was found to be diffusion dependent, as it fits the Higuchi model for drug release (Siepmann and Peppas, 2001). Indeed, the cumulative amount of ibuprofen correlates with the square root of the time ($R^2 > 0.94$) for the first 8 h of incubation for fibres prepared from 1:0 DCM–DMF solutions. Conversely, no linearity was observed for ibuprofen release from P(TMC-CL) fibres prepared from the 3:1 and 6:1 DCM–DMF solutions. It was hypothesized that the presence of DMF in solution could affect the drug distribution within the fibre, leading to a burst release compared with fibres prepared from solutions without DMF. To address this point samples were analyzed using confocal Raman microscopy. To the best of the authors' knowledge this is the first report using confocal Raman microscopy to assess drug distribution in an electrospun fibre. Mapping experiments by confocal Raman allowed screening of specific areas within an electrospun fibre. By using a step slightly smaller than the theoretical size of the spot of the laser beam (0.7 μm), mapping experiments provided the

profiling of all the sample area and discrimination of subtle differences in composition (Adar, [2008](#)). The mapping of the drug in P(TMC-CL) fibres showed that ibuprofen distribution was not completely homogenous. Nevertheless, at the spatial resolution offered by the experimental setup used, no preferential localization of the drug was identified that could be correlated with the burst release (for example, at the fibre edge). In addition, no significant differences were detected when comparing fibres prepared from 1:0 and 3:1 DCM–DMF solutions, suggesting that, at the submicrometer scale, the drug distribution is independent of the solvent mixture applied during electrospinning. The results indicate that other parameters are probably playing a role in ibuprofen release, for example the fibre diameter (Cui *et al.*, [2006](#)). Although no significant differences were detected in terms of mean fibre diameter, the fibre diameter distribution was different between these two types of samples. In fibres prepared from 1:0 DCM–DMF mixtures the presence of a small percentage of fibres with a large diameter ($> 3 \mu\text{m}$) was observed and could have contributed to delaying the release of the drug by increasing the drug diffusion pathway within the polymeric fibre structure.

Owing to the important role of macrophages as effectors of an inflammatory response and as these cells are targets of ibuprofen, primary human monocyte-derived macrophages were selected to evaluate ibuprofen bioactivity after the release from electrospun fibres. Macrophages are highly dynamic and versatile cells, and their response to exogenous stimuli is generally accompanied by alterations in actin assembly/disassembly and cell morphology. These alterations may occur as a consequence of a number of effects such as surface topography (Cao *et al.*, [2010](#)), drugs (Chiou *et al.*, [2003](#)) or soluble factors (Shinji *et al.*, [1991](#); Porcheray *et al.*, [2005](#)). Thus, the effect of ibuprofen-loaded P(TMC-CL) fibres on macrophage morphology was investigated by observing the distribution patterns of cytoskeleton proteins (α -tubulin and F-actin). The results show no major alterations of actin/tubulin cytoskeleton organization in macrophages incubated with ibuprofen or ibuprofen-loaded P(TMC-CL) fibres. However, it cannot be excluded that, to be perceived, considerable alterations would need to have occurred in the heterogeneous macrophage cell population under study. Cells incubated with ibuprofen-loaded P(TMC-CL) fibres secreted less PGE_2 into the cell culture medium than did non-loaded fibres. Although the result did not accomplish the statistical significance ($p = 0.06$) because of the high variability between cell donors, this result strongly suggests that the drug incorporated in the electrospun fibres retains its bioactivity. This result is reinforced by the fact that the percentage of inhibition obtained (47%) is similar to that found with treatment with ibuprofen in solution (56%).

In addition to the classical view of ibuprofen activity, acting on the prostaglandin pathway, there is mounting evidence that lowering levels of eicosanoids is not the only mechanism by which ibuprofen exerts its effects (Stuhlmeier *et al.*, [1999](#); Zhou *et al.*, [2003](#)). Stuhlmeier and co-workers ([1999](#)) showed that ibuprofen can inhibit the nuclear translocation of the nuclear factor kappa B (NF- κ B), a transcription factor critical for the upregulation of expression of pro-inflammatory genes. These reports prompted evaluation of the concentration of pro-inflammatory cytokines (TNF α and IL-6) and an anti-inflammatory cytokine (IL-10) in the cell culture medium in this study. Under the experimental conditions applied in this study, no significant levels of TNF α were found in the cell culture medium. For IL-6 and IL-10, no major differences were found when comparing cytokine levels secreted by cells incubated with ibuprofen-loaded P(TMC-CL) fibres or non-loaded fibres. Similar results were obtained when cells were treated with ibuprofen in the medium (0.1 mg/ml), suggesting that under the set conditions the drug exerts no effect on the cytokine release profile. In the literature divergent effects on cytokine release are ascribed to ibuprofen. Some authors have shown that ibuprofen induces a decrease in the secretion of TNF α and IL-1 β by mononuclear cells (Stuhlmeier *et*

al., [1999](#); Lamanna *et al.*, [2012](#)), whereas a concentration-dependent increase of TNF α and IL-6 has been observed by others (Sirota *et al.*, [2001](#); Lee and Chuang, [2010](#)). Recently, Lamanna and colleagues ([2012](#)) reported the inhibition of TNF α secretion by a macrophage cell line when cells were incubated with a high concentration of ibuprofen (1 mg/ml). However, when applying this concentration, the authors (Lamanna *et al.*, [2012](#)) also found ibuprofen-mediated cytotoxicity and, in agreement with the results of the present study, incubating cells with 0.1 mg/ml of ibuprofen was found to have no effect on IL-6 and TNF α release into the culture medium.

5 Conclusions

Fibres from P(TMC-CL) were successfully prepared by electrospinning. It is shown here that by adjusting the solvent composition, one can change the mean fibre diameter in a controlled manner. An anti-inflammatory drug can be loaded in P(TMC-CL) fibres, the release kinetics being dependent on fibre morphology, which is tuned by the solvent mixture applied for preparation of the electrospinning solution. Ibuprofen was found to maintain its chemical stability and bioactivity after electrospinning, as demonstrated by the fact that the drug was able to reduce the amount of PGE₂ secreted into the cell culture medium by human macrophages. The use of confocal Raman microscopy as a mean to assess the drug distribution within electrospun fibres is also proposed for the first time, being a promising technique to provide new cues on the drug-release process.

The results provide an important insight into the design of a P(TMC-CL)-based nerve conduit combining physical cues provided by the fibres with an anti-inflammatory signalling molecule, which, together, can assist nerve regeneration.

Acknowledgements

This work was financed by FEDER funds through the Programa Operacional Factores de Competitividade – COMPETE and by Portuguese funds through FCT – Fundação para a Ciência e a Tecnologia in the framework of the project PEst-C/SAU/LA0002/2011 and PTDC/CTM-NAN/115124/2009, PTDC/SAU-ONC/112511/2009. L.R.P. thanks FCT for her PhD grant (SFRH / BD / 46015 / 2008) and M.J.O. is a FCT Ciência 2007 fellow. The authors acknowledge Centro de Materiais da Universidade do Porto (CEMUP; REEQ/1062/CTM/2005 from FCT) for the ¹H NMR analysis.

Conflict of interest

The authors have declared that there is no conflict of interest.

REFERENCES

- Adachi K, Yimin Y, Satake K et al. 2005; Localization of cyclooxygenase-2 induced following traumatic spinal cord injury. *Neurosci Res* 51 :73-80.
- Adar F. 2008; Raman images from raman maps – spatial resolution, mapping speed, and multivariate techniques for constructing the image. *Spectroscopy* 23 : 14 – 21.
- Agarwal S, Wendorff JH, Greiner A. 2009; Progress in the field of electrospinning for tissue engineering applications. *Adv Mater* 21: 3343–3351.
- Bölgren N, Menceloglu YZ, Acatay K, Vargel I, Piskin E. 2005; In vitro and in vivo degradation of non-woven materials made of poly(ϵ -caprolactone) nanofibres prepared by electrospinning under different conditions. *J Biomater Sci Polym Ed* 16: 1537–1555.
- Brodbeck WG, Nakayama Y, Matsuda T et al. 2002; Biomaterial surface chemistry dictates adherent monocyte/macrophage cytokine expression in vitro. *Cytokine* 18: 311–319.
- Cao H, McHugh K, Chew SY et al. 2010; The topographical effect of electrospun nanofibrous scaffolds on the in vivo and in vitro foreign body reaction. *J Biomed Mater Res A* 93: 1151–1159.
- Casha S, Zygun D, McGowan MD et al. 2012; Results of a phase II placebo-controlled randomized trial of minocycline in acute spinal cord injury. *Brain* 135: 1224–1236.
- Chan CC. 2008; Inflammation: beneficial or detrimental after spinal cord injury? *Recent Pat CNS Drug Discov* 3: 189–199.
- Chew SY, Wen J, Yim EKF et al. 2005; Sustained release of proteins from electrospun biodegradable fibres. *Biomacromolecules* 6: 2017–2024.
- Chiou WF, Shum AYC, Peng CH et al. 2003; Piperlactam S suppresses macrophage migration by impeding F-actin polymerization and filopodia extension. *Eur J Pharmacol* 458: 217–225.
- Corey JM, Lin DY, Mycek KB et al. 2007; Aligned electrospun nanofibres specify the direction of dorsal root ganglia neurite growth. *J Biomed Mater Res A* 83: 636–645.
- Cui W, Li X, Zhu X et al. 2006; Investigation of drug release and matrix degradation of electrospun poly(DL-lactide) fibres with paracetamol inoculation. *Biomacromolecules* 7: 1623–1629.
- Fitch MT, Silver J. 2008; CNS injury, glial scars, and inflammation: Inhibitory extracellular matrices and regeneration failure. *Exp Neurol* 209: 294–301. Formhals A. 1934; US patent (1,975,504).
- Han J, Branford-White CJ, Zhu LM. 2010; Preparation of poly(ϵ -caprolactone)/ poly(trimethylene carbonate) blend nanofibres by electrospinning. *Carbohydr Polym* 79: 214–218.
- Heikkilä P, Harlin A. 2008; Parameter study of electrospinning of polyamide-6. *Eur Polym J* 44: 3067–3079.
- Hsu CM, Shivkumar S. 2004; N,N-dimethylformamide additions to the solution for the electrospinning of poly(ϵ -caprolactone) nanofibres. *Macromol Mater Eng* 289: 334–340.
- Hurtado A, Cregg JM, Wang HB et al. 2011; Robust CNS regeneration after complete spinal cord transection using aligned poly-L-lactic acid microfibrils. *Biomaterials* 32: 6068–6079.
- Jia YT, KimHY, Gong J et al. 2006; Electrospun nanofibres of block copolymer of trimethylene carbonate and ϵ -caprolactone. *J Appl Polym Sci Symp* 99: 1462–1470.
- Jiang X, Mi R, Hoke A et al. 2012; Nanofibrous nerve conduit-enhanced peripheral nerve regeneration. *J Tissue Eng Regen Med*. DOI: 10.1002/term.1531. [Epub ahead of print]

- KimK, Luu YK, Chang C et al. 2004; Incorporation and controlled release of a hydrophilic antibiotic using poly(lactide-co-glycolide)- based electrospun nanofibrous scaffolds. *J Control Release* 98: 47–56.
- Lamanna G, Russier J, Dumortier H et al. 2012; Enhancement of anti-inflammatory drug activity by multivalent adamantanebased dendrons. *Biomaterials* 33: 5610–5617.
- Lee YJ, Chuang YC. 2010; Ibuprofen augments pro-inflammatory cytokine release in a mouse model of *Vibrio vulnificus* infection. *Microbiol Immunol* 54: 542–550. Lee YS, Arinze TL. 2011; Electrospun nanofibrous materials for neural tissue engineering. *Polymers* 3: 413–426.
- Liu T, Xu J, Chan BP et al. 2012; Sustained release of neurotrophin-3 and chondroitinase ABC from electrospun collagen nanofibre scaffold for spinal cord injury repair. *J Biomed Mater Res A* 100A: 236–242.
- Ma W, St-Jacques B, Cruz Duarte P. 2012; Targeting pain mediators induced by injured nerve-derived COX₂ and PGE₂ to treat neuropathic pain. *Expert Opin Ther Targets* 16: 527–540.
- Martins A, Araújo JV, Reis RL et al. 2007; Electrospun nanostructured scaffolds for tissue engineering applications. *Nanomedicine* 2: 929–942.
- Mitchell JA, Akarasereenont P, Thiemermann C et al. 1993; Selectivity of nonsteroidal antiinflammatory drugs as inhibitors of constitutive and inducible cyclooxygenase. *Proc Natl Acad Sci USA* 90:11693–11697.
- Natu MV, de Sousa HC, Gil MH. 2010; Effects of drug solubility, state and loading on controlled release in bicomponent electrospun fibres. *Int J Pharm* 397: 50–58.
- Oliveira MI, Santos SG, Oliveira MJ et al. 2012; Chitosan drives anti-inflammatory macrophage polarisation and proinflammatory dendritic cell stimulation. *Eur Cell Mater* 24: 136–153.
- Pêgo AP, Poot AA, Grijpma DW et al. 2001; Copolymers of trimethylene carbonate and epsilon-caprolactone for porous nerve guides: Synthesis and properties. *J Biomater Sci Polym Ed* 12: 35–53.
- Pêgo AP, Poot AA, Grijpma DW et al. 2003; Biodegradable elastomeric scaffolds for soft tissue engineering. *J Control Release* 87: 69–79.
- Porcheray F, Viaud S, Rimaniol AC et al. 2005; Macrophage activation switching: an asset for the resolution of inflammation. *Clin Exp Immunol* 142: 481–489.
- Rainsford KD. 2009; Ibuprofen: pharmacology, efficacy and safety. *Inflammopharmacology* 17: 275–342.
- Schaub NJ, Gilbert RJ. 2011; Controlled release of 6-aminonicotinamide from aligned, electrospun fibres alters astrocyte metabolism and dorsal root ganglia neurite outgrowth. *J Neural Eng* 8: 046026.
- Schwartz M, London A, Shechter R. 2009; Boosting T-cell immunity as a therapeutic approach for neurodegenerative conditions: The role of innate immunity. *Neuroscience* 158: 1133–1142.
- Shinji H, Kaiho S, Nakano T et al. 1991; Reorganization of microfilaments in macrophages after LPS stimulation. *Exp Cell Res* 193: 127–133.
- Siepmann J, Peppas NA. 2001; Modeling of drug release from delivery systems based on hydroxypropyl methylcellulose (HPMC). *Adv Drug Deliv Rev* 48: 139–157.
- Sirota L, Shacham D, Punsky I et al. 2001; Ibuprofen affects pro- and antiinflammatory cytokine production by mononuclear cells of preterm newborns. *Biol Neonate* 79: 103–108.
- Stuhlmeier KM, Li H, Kao JJ. 1999; Ibuprofen: New explanation for an old phenomenon. *Biochem Pharmacol* 57: 313–320.
- Thuret S, Moon LDF, Gage FH. 2006; Therapeutic interventions after spinal cord injury. *Nat Rev Neurosci* 7: 628–643.



- Tungprapa S, Jangchud I, Supaphol P. 2007; Release characteristics of four model drugs from drug-loaded electrospun cellulose acetate fibre mats. *Polymer* 48: 5030–5041.
- Vleggeert-Lankamp CLAM, Wolfs J, Pêgo AP et al. 2008; Effect of nerve graft porosity on the refractory period of regenerating nerve fibres: laboratory investigation. *J Neurosurg* 109: 294–305.
- Xie J, MacEwan MR, Schwartz AG et al. 2010; Electrospun nanofibres for neural tissue engineering. *Nanoscale* 2: 35–44.
- Yao L, O'Brien N, Windebank A et al. 2009; Orienting neurite growth in electrospun fibrous neural conduits. *J Biomed Mater Res B Appl Biomater* 90: 483–491.
- Yu W, Zhao W, Zhu C et al. 2011; Sciatic nerve regeneration in rats by a promising electrospun collagen/poly(ϵ -caprolactone) nerve conduit with tailored degradation rate. *BMC Neurosci* 12: 68.
- Zhao P, Waxman SG, Hains BC. 2007; Extracellular signal-regulated kinase-regulated microglia-neuron signaling by prostaglandin E₂ contributes to pain after spinal cord injury. *J Neurosci* 27: 2357–2368.
- Zhou Y, Su Y, Li BL et al. 2003; Nonsteroidal anti-inflammatory drugs can lower amyloidogenic A β (42) by inhibiting Rho. *Science* 302: 1215–1217.

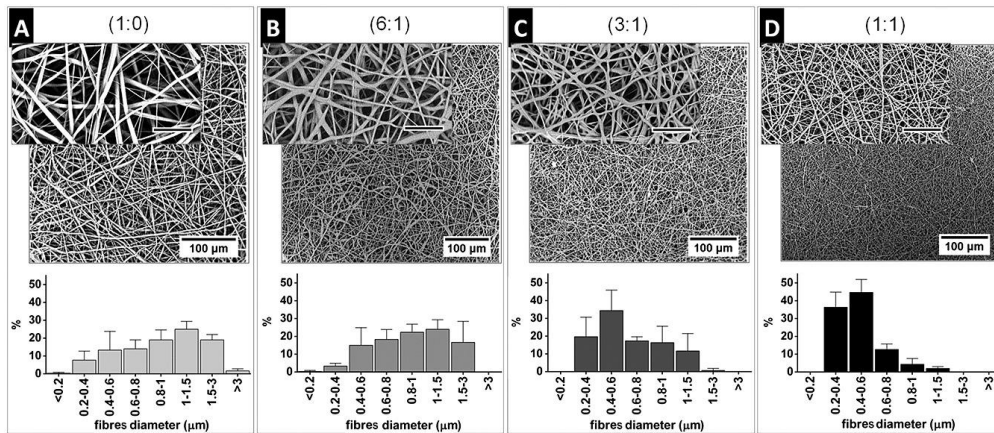


Figure 1. Representative scanning electron microscopy photomicrographs of poly(trimethylene carbonate-co- ϵ -caprolactone) [P(TMC-CL)] fibres and fibre diameter distribution ($n = 3$). Samples were prepared using P(TMC-CL) solutions in a dichloromethane (DCM)-*N,N*-dimethylformamide (DMF) mixture with increasing amounts of DMF: (A) 1:0 DCM-DMF; (B) 6:1 DCM-DMF; (C) 3:1 DCM-DMF; (D) 1:1 DCM-DMF. Higher magnification images scale bar = 20 μm

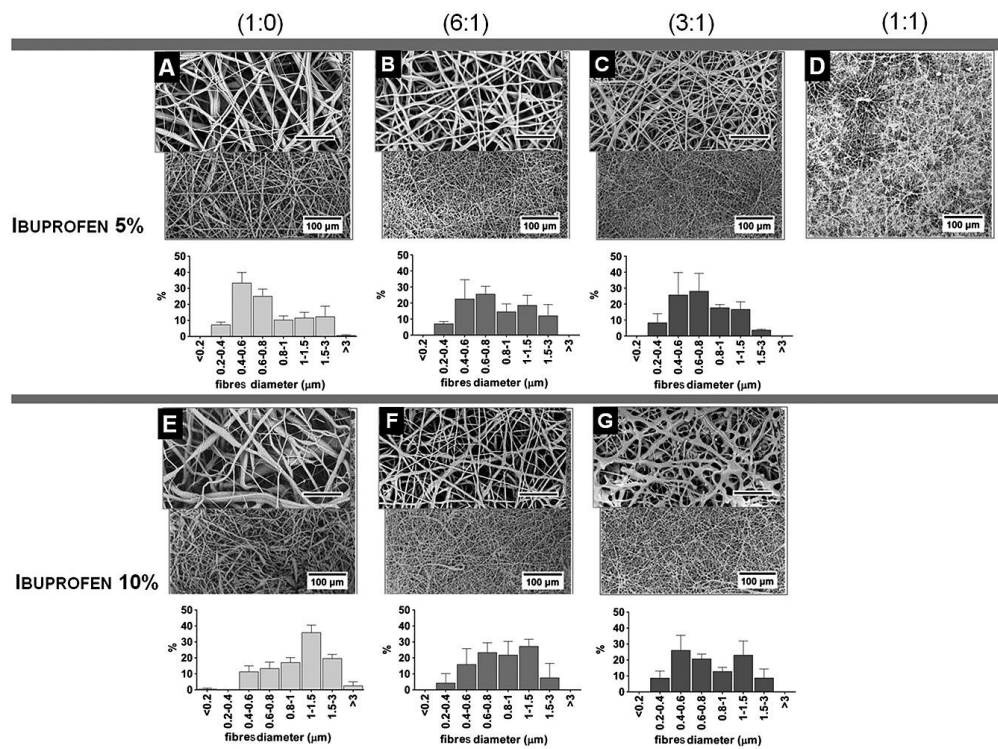


Figure 2. Scanning electron microscopy photomicrographs of ibuprofen-loaded poly(trimethylene carbonate-co- ϵ -caprolactone) [P(TMC-CL)] fibres and respective fibre diameter distribution ($n = 3$). Fibres were obtained from solutions containing 5% (A–D) and 10% (E–G) of ibuprofen (w/w of polymer) and applying different dichloromethane (DCM)–*N,N*-dimethylformamide (DMF) mixtures as solvent: (A,E) 1:0 DCM–DMF; (B,F) 6:1 DCM–DMF; (C,G) 3:1 DCM–DMF; (D) 1:1 DCM–DMF. Higher magnification images scale bar = 20 μ m

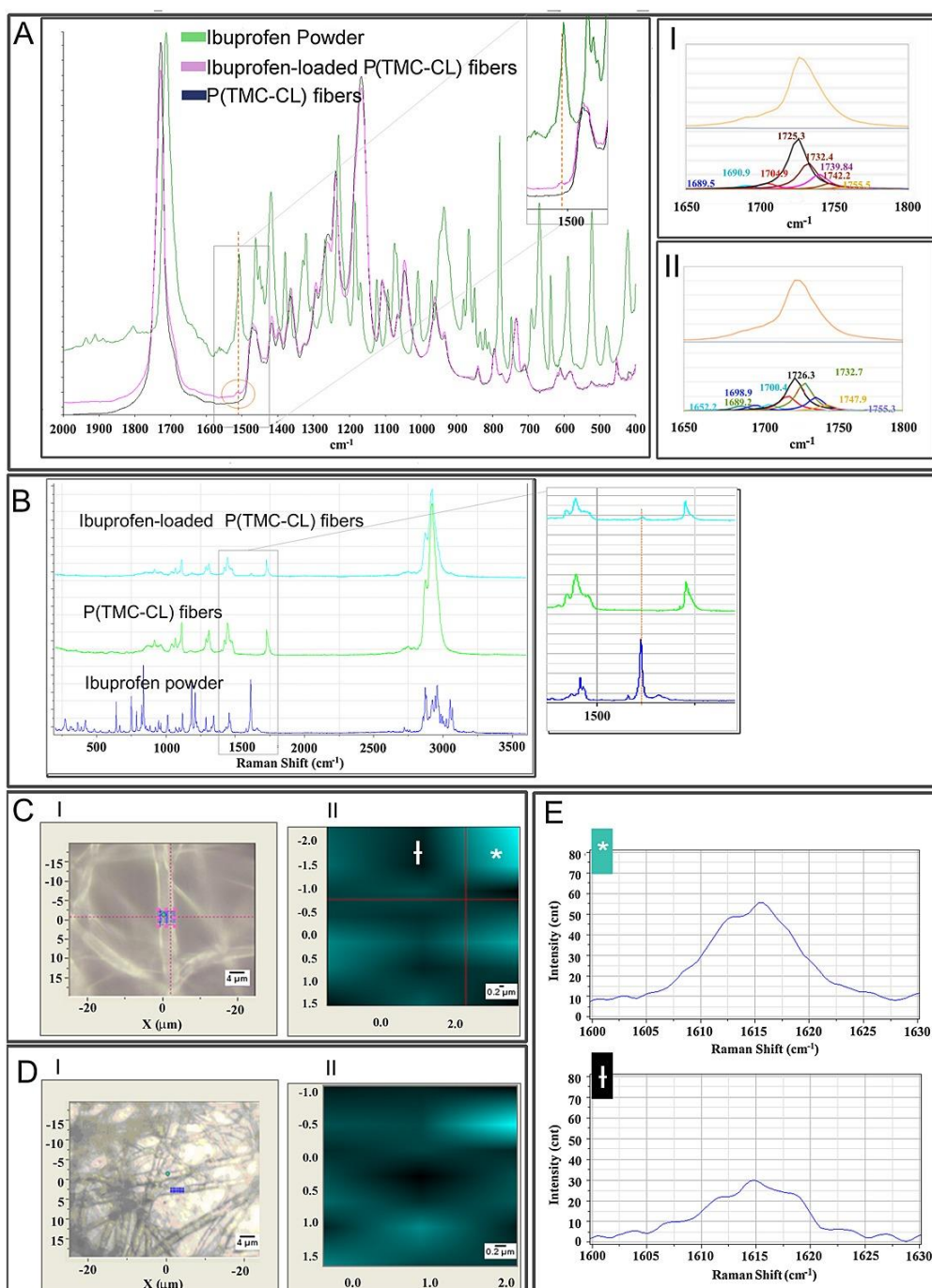


Figure 3. (A) Attenuated total reflectance–Fourier transform infrared spectroscopy spectrum of ibuprofen-loaded poly(trimethylene carbonate-co- ϵ -caprolactone) [P(TMC-CL)] fibres prepared from 1:0 dichloromethane (DCM)–*N,N*-dimethylformamide (DMF) solutions (pink). The spectra of ibuprofen (in green) and non-loaded fibres (blue) is shown for comparison. Curve fitting in the spectral region between 1670/cm and 1800/cm of (I) P(TMC-CL) fibres and (II) ibuprofen-loaded P(TMC-CL) fibres. (B) Raman spectra of ibuprofen (dark blue), P(TMC-CL) fibres (green), and ibuprofen-loaded P(TMC-CL) fibres (light blue) obtained from 1:0 DCM–DMF solutions. (C,D) Confocal Raman microscopy analysis of ibuprofen-loaded P(TMC-CL) fibres. (I) In images blue indicates the region analysed from ibuprofen-loaded P(TMC-CL) fibres prepared from (C) 1:0 DCM–DMF and (D) 3:1 DCM–DMF solutions, respectively

(axis indicates distance in μm). (II) For each sample the mapping of the 1610/cm ibuprofen Raman band relative to background bands (1510–1525/cm and 1645–1665/cm; axis indicates distance in μm) is presented. These are representative images from three different areas analysed. The overlay of the spectra obtained for each point is presented in Figure S3 (see Supporting Information). Regions with high concentration of ibuprofen are depicted in bright green (*) and regions with lower concentration are depicted in dark green (+). (E) Representative spectra of these regions are shown

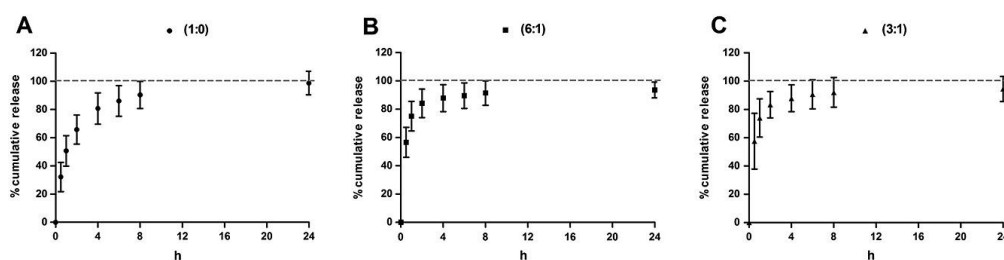


Figure 4. Cumulative release of ibuprofen from poly(trimethylene carbonate-co- ϵ -caprolactone) [P(TMC-CL)] fibres in phosphate-buffered saline (PBS) (37 °C). Samples were prepared from (A) 1:0 dichloromethane (DCM)–*N,N*-dimethylformamide (DMF), (B) 6:1 DCM–DMF and (C) 3:1 DCM–DMF solutions containing 5% ibuprofen (w/w of polymer). Fibre concentration in PBS was 5 mg/ml ($n = 9$)

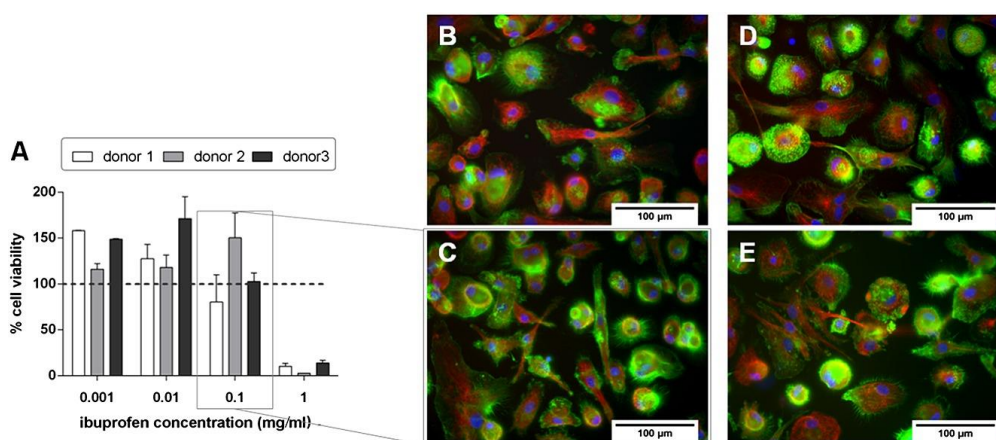


Figure 5. (A) Macrophage viability when incubated for 72 h with ibuprofen at different concentrations. The percentage of viable cells was calculated relative to cells treated with ibuprofen solvent (ethanol 70% v/v). Bars represent mean values and error bars show standard deviation. Results are representative of three independent experiments. (B–E) Actin–tubulin cytoskeleton immunolabelling of macrophages. Macrophages were incubated for 72 h in the presence of (B) ethanol 70% (v/v), (C) ibuprofen 0.1 mg/ml, (D) poly(trimethylene carbonate-co- ϵ -caprolactone) [P(TMC-CL)] fibres, and (E) ibuprofen-loaded P(TMC-CL) fibres. Scale bar = 100 μm . α -Tubulin is shown in red, F-actin in green and the cell nucleus in blue. Magnified images of each condition are also presented (scale bar = 20 μm)

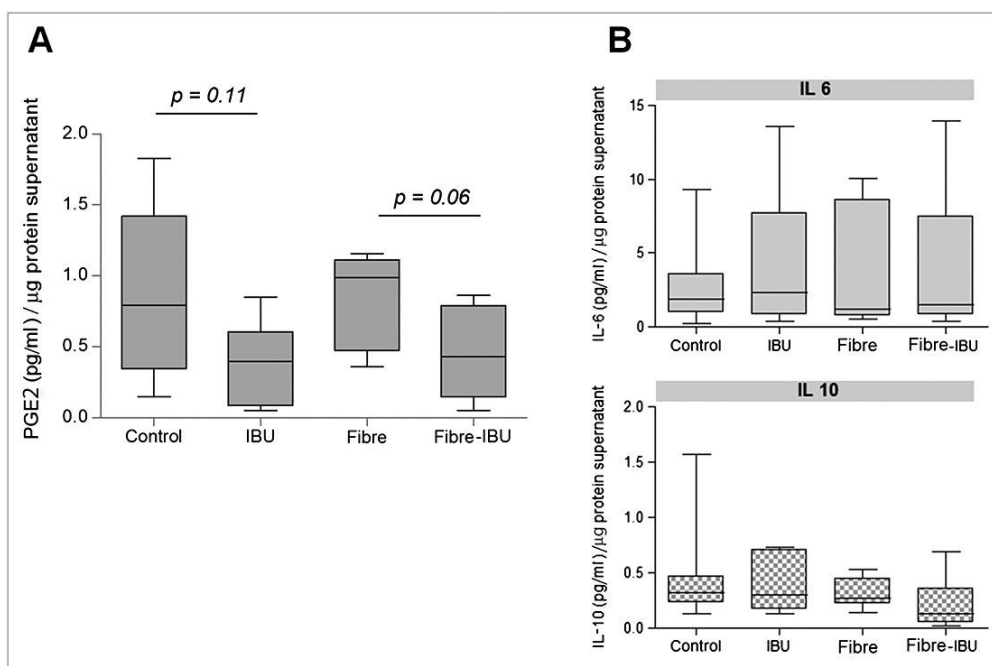


Figure 6. Effect of ibuprofen on (A) prostaglandin E₂ (PGE₂) and (B) cytokine [interleukin (IL)-6 and IL-10] release by human macrophages. Results are expressed as box-whisker plots showing the quantification of (A) PGE₂ or (B) IL-6 and IL-10 released into the cell culture medium after 72 h in contact with soluble ibuprofen added in solution to the cell culture medium or released from P(TMC-CL) electrospun fibres. The P(TMC-CL) fibres were prepared from 1:0 dichloromethane (DCM)-*N,N*-dimethylformamide (DMF) solutions. Cells incubated with non-loaded fibres (Fibre) or with ibuprofen (IBU) solvent (ethanol 70% v/v, Control) were used as controls. Results were obtained from cells from five independent donors and seven samples and are normalized by the total amount of protein in the supernatant. The *p*-value calculated by *t*-test

Table 1. Poly(trimethylene carbonate-co-ε-caprolactone) [P(TMC-CL)] electrospun fibre diameters

	Fibre diameter (µm)			
	1:0 DCM-DMF	6:1 DCM-DMF	DCM:DMF (3:1)	1:1 DCM-DMF
Non-loaded	1.09 ± 0.10	1.02 ± 0.19	0.67 ± 0.12	0.48 ± 0.03
Ibuprofen 5%	0.84 ± 0.08	0.91 ± 0.09	0.76 ± 0.06	–
Ibuprofen 10%	1.2 ± 0.05	0.91 ± 0.2	0.84 ± 0.12	–

Mean diameter ± standard deviation (*n* = 3) of P(TMC-CL) fibres prepared from dichloromethane (DCM)-*N,N*-dimethylformamide (DMF) solutions at ratios of 1:0, 6:1, 3:1 and 1:1 in the absence or presence of 5% and 10% of ibuprofen (w/w of polymer), respectively. Standard deviation represents variability between different samples.

Supporting Information

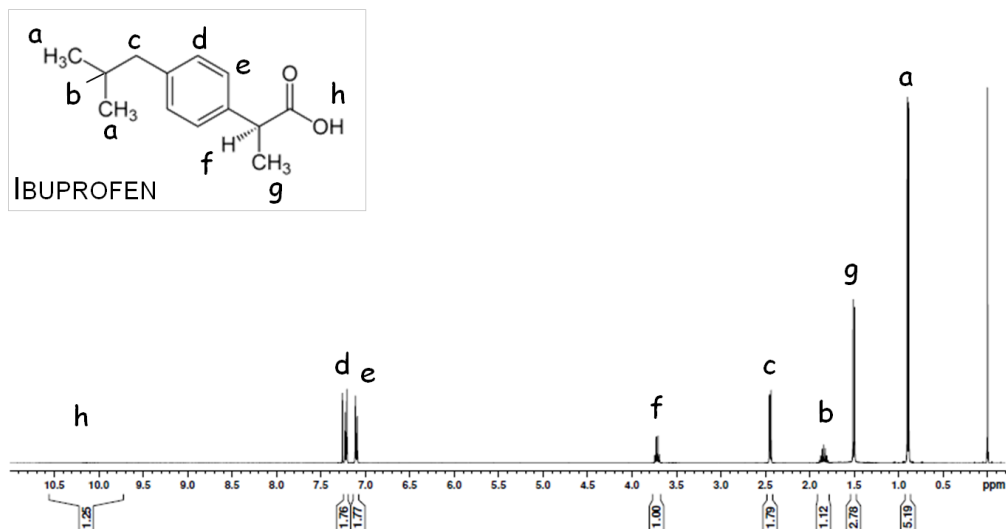


Figure S1. ^1H NMR spectrum of ibuprofen-loaded P(TMC-CL) fibers, showing the identification of ibuprofen characteristic peaks.

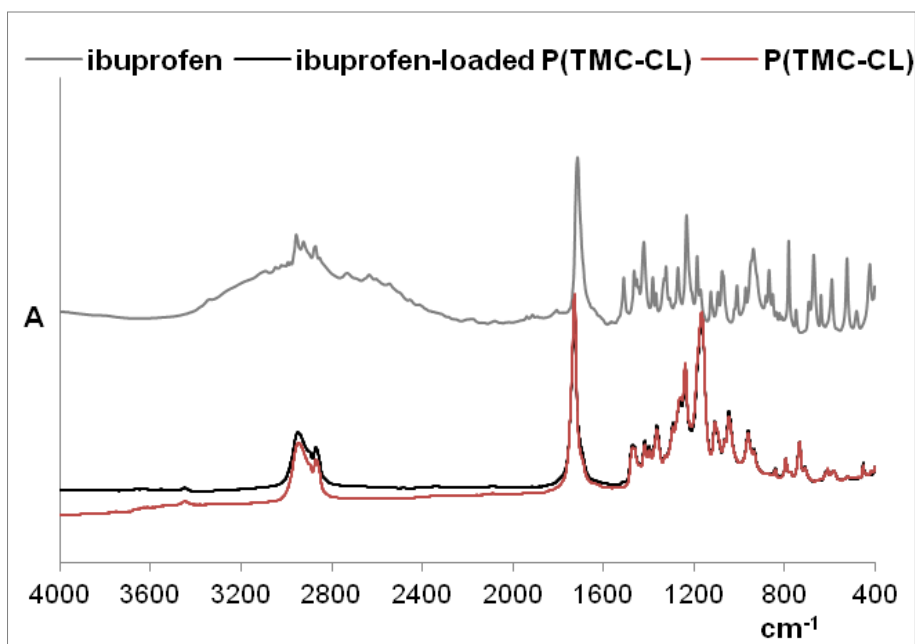


Figure S2. Full ATR-FTIR spectrum of ibuprofen (grey), ibuprofen-loaded P(TMC-CL) fibers (black) and P(TMC-CL) (red).

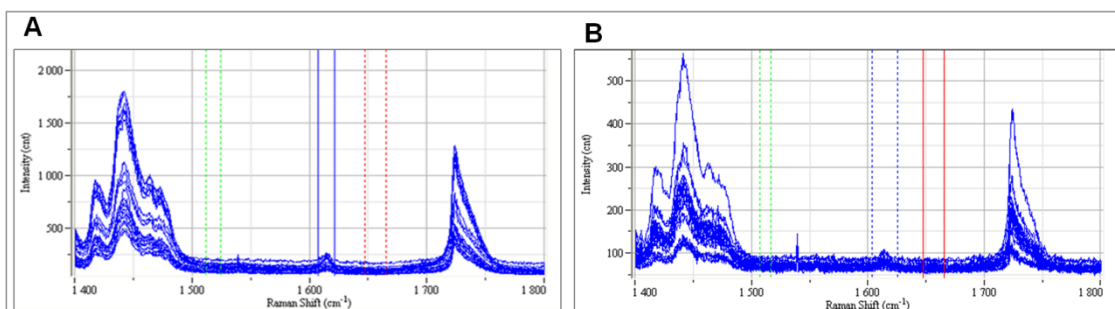


Figure S3. Overlay of spectra obtained from mapping experiments of ibuprofen-loaded P(TMC-CL) fibers prepared from (A) DCM:DMF (1:0) and (B) DCM:DMF (3:1) solutions.

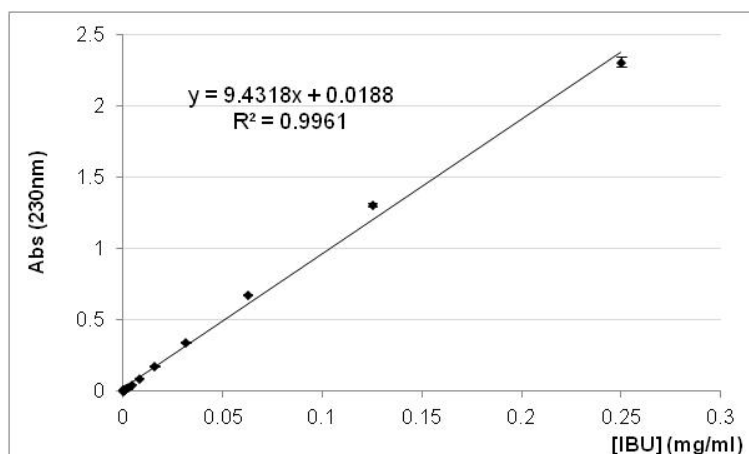


Figure S4. Standard calibration curve obtained for ibuprofen.

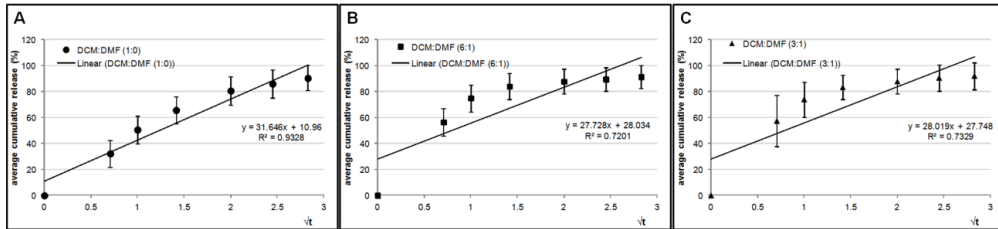


Figure S5. Fittings according to Higuchi model for drug release for fibers prepared from (A) DCM:DMF (1:0), (B) DCM:DMF (6:1) and (C) DCM:DMF (3:1)

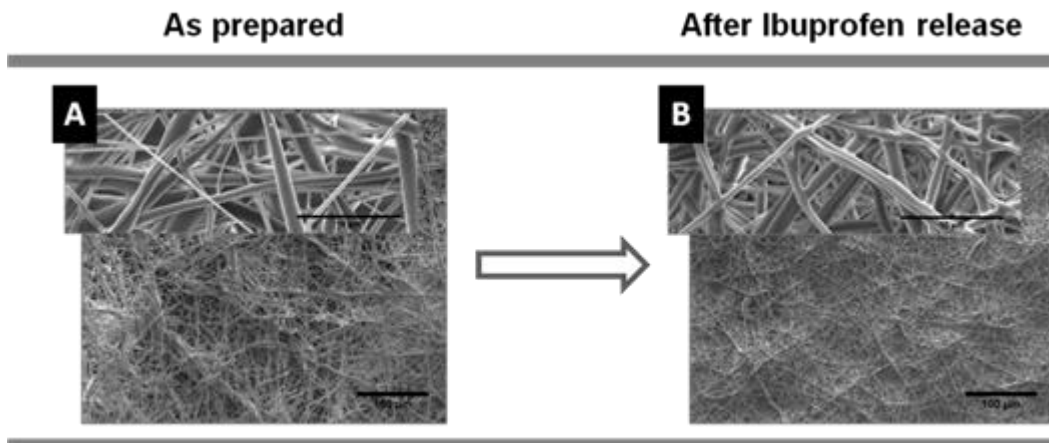


Figure S6. SEM micrographs of ibuprofen-loaded P(TMC-CL) fibers prepared from DCM:DMF (1:0) solution (A) before and (B) after ibuprofen release.

1. Crettaz von Roten, F., Public perceptions of animal experimentation across Europe. *Public Understanding of Science*, 2012.
2. Aldhous, P., A. Coghlan, and J. Copley, Animal experiments: let the people speak. . *New Scientist.*, 1999 162(2187): p. 26-31.
3. European Commission, Seventh Report on the Statistics on the Number of Animals used for Experimental and other Scientific Purposes in the Member States of the European Union. 2013: Brussels.
4. Eurostat, Europe in Figures - Eurostat yearbook 2012. 2012, Publications Office of the European Union: Luxembourg. p. 119.
5. Eurostat (2009) EU cattle, pigs, sheep and goats: monthly slaughter statistics in 2008. *Data in focus 15/2009*.
6. Eurostat (2008) Poultry statistics in the European Union: flock numbers, hatcheries, trade and slaughterings. *Data in focus 31/2008*.
7. Eurostat, Fishery Statistics, in Agriculture and fishery statistics - Main results 2010-11. 2011, Publications Office of the European Union: Luxembourg.
8. Cohen, C., The Case for the Use of Animals in Biomedical Research. *New England Journal of Medicine*, 1986. 315(14): p. 865-870.
9. Dell, R.B., S. Holleran, and R. Ramakrishnan, Sample size determination. *ILAR J*, 2002. 43(4): p. 207-13.
10. Bloomsmith, M.A., S.J. Schapiro, and E.A. Strobart, Preparing chimpanzees for laboratory research. *ILAR J*, 2006. 47(4): p. 316-25.
11. Davis, S.L., et al., Noninvasive pulmonary [18F]-2-fluoro-deoxy-D-glucose positron emission tomography correlates with bactericidal activity of tuberculosis drug treatment. *Antimicrob Agents Chemother*, 2009. 53(11): p. 4879-84.
12. Davis, S.L., et al., Bacterial Thymidine Kinase as a Non-Invasive Imaging Reporter for Mycobacterium tuberculosis in Live Animals. *PLoS ONE*, 2009. 4(7): p. e6297.
13. Andreu, N., P.T. Elkington, and S. Wiles, Molecular Imaging in TB: From the Bench to the Clinic, in *Understanding Tuberculosis - Global Experiences and Innovative Approaches to the Diagnosis*, P.-J. Cardona, Editor. 2012, InTech.
14. Morton, D.B., Humane endpoints in animal experimentation for biomedical research, in *Humane endpoints in animals experiments for biomedical research*, C.F.M. Hendriksen and D.B. Morton, Editors. 1999, Royal Society of Medicine Press: London. p. 5-12.



15. Van Loo, P.L.P., et al., Preference for social contact versus environmental enrichment in male laboratory mice. *Laboratory Animals*, 2004. 38(2): p. 178-188.
16. Van Loo, P.L.P., L.F.M. Van Zutphen, and V. Baumans, Male management: coping with aggression problems in male laboratory mice. *Laboratory Animals*, 2003. 37(4): p. 300-313.
17. Beery, A.K. and I. Zucker, Sex bias in neuroscience and biomedical research. *Neuroscience & Biobehavioral Reviews*, 2011. 35(3): p. 565-572.
18. Wald, C. and C. Wu, Of Mice and Women: The Bias in Animal Models. *Science*, 2010. 327(5973): p. 1571-1572.
19. Hawkins, P., et al., Husbandry refinements for rats, mice, dogs and non-human primates used in telemetry procedures. Seventh report of the BVAAWF/FRAME/RSPCA/UFAW Joint Working Group on Refinement, Part B. *Lab Anim*, 2004. 38(1): p. 1-10.
20. Weekley, L.B., P. Guittin, and G. Chamberland, The international symposium on regulatory testing and animal welfare: recommendations on best scientific practices for safety evaluation using nonrodent species. *ILAR J*, 2002. 43 Suppl: p. S118-22.
21. Stephens, M.L., et al., Possibilities for refinement and reduction: future improvements within regulatory testing. *ILAR J*, 2002. 43 Suppl: p. S74-9.
22. Broadhead, C.L., et al., Prospects for reducing and refining the use of dogs in the regulatory toxicity testing of pharmaceuticals. *Hum Exp Toxicol*, 2000. 19(8): p. 440-7.
23. Jennings, M., et al., Refinements in husbandry, care and common procedures for non-human primates: Ninth report of the BVAAWF/FRAME/RSPCA/UFAW Joint Working Group on Refinement. *Lab Anim*, 2009. 43 Suppl 1: p. 1-47.
24. Morton, D.B., et al., Refinements in telemetry procedures: seventh report of the BVA(AWF)/FRAME/RSPCA/UFAW joint working group on refinement, part A. *Laboratory Animals*, 2003. 37: p. 261-99.
25. Kramer, K. and L.B. Kinter, Evaluation and applications of radiotelemetry in small laboratory animals. *Physiological Genomics*, 2003. 13(3): p. 197-205.
26. Turner, P.V., et al., Refinements in the Care and Use of Animals in Toxicology Studies Regulation, Validation, and Progress. *Journal of the American Association for Laboratory Animal Science*, 2003. 42(6): p. 8-15.
27. European Commission, Directive 2010/63/EU of the European Parliament and of the Council of 22 September 2010 on the protection of animals used for scientific purposes, E. Commission, Editor. 2010, Official Journal of the European Union: Brussels. p. 33-79.
28. Franco, N. and I. Olsson, Scientists and the 3Rs: attitudes to animal use in biomedical research and the effect of mandatory training in laboratory animal science. *Laboratory animals*, 2014. 48(1): p. 50-60.
29. Franco, N.H., M. Magalhães-Sant'Ana, and I.A.S. Olsson, Welfare and quantity of life, in Dilemmas in Animal Welfare, M. Appleby, D. Weary, and P. Sandøe, Editors. 2014, CABI: Oxfordshire. p. 46-66.
30. Wolfensohn, S., Euthanasia and Other Fates for Laboratory Animals, in *The UFAW Handbook on the Care and Management of Laboratory and Other Research Animals*, R. Hubrecht and J. Kirkwood, Editors. 2010, Wiley-Blackwell. p. 219-226.
31. Kerwin, A.M., Overcoming the Barriers to the Retirement of Old and New World Monkeys From Research Facilities. *Journal of Applied Animal Welfare Science*, 2006. 9(4): p. 337-347.
32. Waitt, C.D., M. Bushnitz, and P.E. Honess (2010) Designing Environments for Aged Primates. *Laboratory Primate Newsletter* 49.
33. Carbone, L. (1997) Adoption of Research Animals. *Animal Welfare Information Center Newsletter* 7.

34. DiGangi, B.A., P.C. Crawford, and J.K. Levy, Outcome of Cats Adopted From a Biomedical Research Program. *Journal of Applied Animal Welfare Science*, 2006. 9(2): p. 143-163. 35. Doehring, D. and M.H. Erhard, [Whereabouts of surplus and surviving laboratory animals]. *ALTEX*, 2005. 22(1): p. 7-11.
36. LASA, LASA Guidance on the Rehoming of Laboratory Dogs. A report based on a LASA working party and LASA meeting on rehoming laboratory animals, M. Jennings and B. Howard, Editors. 2004.
37. Taylor, K., The need for proactive rehoming policies in the EU. *ALTEX Proceedings*, 2015. 4(2): p. 228.
38. Kelch, T.G., Constitutional Protection for Animals, in *Globalization and Animal Law: Comparative Law, International Law and International Trade*. 2011, Kluwer Law International. p. 271-292.
39. Tierschutzgesetz. (TierSchG). (Animal Protection Act). December 9th 2010: BGBl. I S. 1934.
40. Franco, N.H., M. Correia-Neves, and I.A.S. Olsson, Animal welfare in studies on murine tuberculosis: assessing progress over a 12-year period and the need for further improvement. *PloS one*, 2012. 7(10): p. e47723.
41. Pereira, S. and M. Tettamanti, Ahimsa and alternatives - The concept of the 4th R. The CPCSEA in India. *ALTEX*, 2005. 22(1): p. 3-6.
42. Franco, N.H., Animal Experiments in Biomedical Research: A Historical Perspective. *Animals*, 2013. 3(1): p. 238-273.
43. Kant, I., *Lectures on Ethics*, J.B. Schneewind, Editor. 1997 [1780], Cambridge University Press.
44. Singer, P., *Animal Liberation*. 2002: Ecco.
45. Boralevi, L.C., Bentham and the Oppressed. 1984: W. de Gruyter.
46. McMahan, J., Eating animals the nice way. *Daedalus*, 2008. 137(1): p. 66-76.
47. Russell, W.M.S. and R.L. Burch, *The principles of humane experimental technique* 1959, London: Methuen & Co. Ltd.
48. de Boo, M.J., et al., The interplay between replacement, reduction and refinement: considerations where the Three Rs interact. *Animal Welfare*, 2005. 14(4): p. 327-332.
49. Hansen, A.K., et al., The need to refine the notion of reduction, in *Humane endpoints in animal experiments for biomedical research*, C. Hendriksen and D. Morton, Editors. 1999, RSM Press: London. p. 139-144.
50. Frey, R.G., Utilitarianism and Animals, in *The Oxford Handbook of Animal Ethics*, T.L. Beauchamp and R.G. Frey, Editors. 2011, OUP USA. p. 172-197.
51. McMahan, J., The Wrongness of Killing and the Badness of Death, in *The Ethics of Killing: Killing at the Margins of Life*. 2002, Oxford University Press. p. 189-202.
52. Rollin, B., Death, telos and euthanasia, in *The end of animal life: a start for ethical debate.* , F.L.B. Meijboom and E.N. Stassen, Editors. 2016, Wageningen Academic Publishers: Wageningen.
53. Rollin, B.E., Animal Rights as a Mainstream Phenomenon. *Animals*, 2011. 1(1): p. 102-115.
54. Iliff, S.A., An Additional "R": Remembering the Animals. *ILAR Journal*, 2002. 43(1): p. 38-47.
55. Calhoun, J.B., *The Ecology and Sociology of the Norway Rat*. 1963: U.S. Government Printing Office.
56. Altun, M., et al., Behavioral impairments of the aging rat. *Physiology & Behavior*, 2007. 92(5): p. 911-923.
57. Holmberg, T., A Feeling for the Animal: On Becoming an Experimentalist. *Society and Animals*, 2008. 16 p. 316-335
58. Bayne, K., Development of the human-research animal bond and its impact on animal well-being. *ILAR J*, 2002. 43(1): p. 4-9.



59. Chang, F.T. and L.H. Hart, Human-animal bonds in the laboratory: how animal behavior affects the perspectives of caregivers. *ILAR J*, 2002. 43(1): p. 10-8.
60. Cressey, D., *Battle Scars*. Nature, 2011. 470: p. 452-453.
61. Arluke, A., *Managing emotions in an animal shelter*. 1994: Animals and human society. New York: Routledge.
62. Birke, L., A. Arluke, and M. Michael, The division of Emotional Labor, in *The Sacrifice: How Scientific Experiments Transform Animals and People*. 2007, Purdue University Press. p. 93-110.
63. Lynch, M.E., *Sacrifice and the Transformation of the Animal Body into a Scientific Object: Laboratory Culture and Ritual Practice in the Neurosciences*. *Social Studies of Science*, 1988. 18(2): p. 265-289.
64. Arluke, A. and C.R. Sanders, *Regarding Animals*. 1996: Temple University Press.
65. Baumans, V., et al., eds. *Making Lives Easier for Animals in Research Labs*. 2007, Animal Welfare Institute: Washington.
66. Huddart, S. and C. Naherniak, *Animals in the Classroom*, in *Teaching Green: The Elementary Years : Hands-on Learning in Grades K-5*, T. Grant and G. Littlejohn, Editors. 2005, New Society Publishers: Toronto. p. 101-107.
67. Fonseca, M.J., et al., *Children's attitudes towards animals: evidence from the RODENTIA project*. *Journal of Biological Education*, 2011. 45(3): p. 121-128.
68. Hubrecht, R., *Comfortable quarters for laboratory dogs in research institutions*, in *Comfortable quarters for laboratory animals*, V. Reinhardt and A. Reinhardt, Editors. 2002, Animal Welfare Institute. p. 56-64.